Proceedings 10th NUMGE 2023
10th European Conference on Numerical Methods in Geotechnical Engineering
Zdravkovic L, Kontoe S, Taborda DMG, Tsiampousi A (eds)

https://doi.org/10.53243/NUMGE2023-346

Stability analysis of TSFs using a simplified quasi-1D deformation model

K. Bernardo[1,2], F. L. Rivarola[1,2], A. O. Sfriso[1,2]
[1]*SRK Consulting, Buenos Aires, Argentina*
[2]*Universidad de Buenos Aires, Buenos Aires, Argentina*

ABSTRACT: The assessment of risk of static liquefaction of tailings storage facilities (TSF) has become a key topic in recent years. The stability of upstream-raised tailings dams relies on the strength of brittle, strain-softening tailings and therefore cannot be analysed with standard limit equilibrium (LE) tools that do not account for progressive failure. Finite element models (FEM), on the other hand, can capture the complete material behaviour, but require data that is usually unavailable during screening analyses at scoping study level. It is therefore convenient to use simple tools providing insight into the expected TSF behaviour before running full FEM models. This paper describes a simplified procedure to analyse the stability of tailings storage facilities at screening level, employing a quasi-1D FEM model. NorSand critical state constitutive model was employed. The procedure allows for the simulation of the entire construction sequence, including raises at a prescribed rate and water content, evaporation and infiltration, consolidation, and time effects. At any time, a simple, static pushover analysis is used to assess the stability of the column and to identify weak points. The proposed strategy reproduces the key features of tailings behaviour along the relevant stress paths, estimates the brittleness of tailings at various depths, and produces an assessment of the risk of static liquefaction for various deposition strategies and water flow scenarios.

Keywords: Liquefaction; TSF; Plaxis 2D; NorSand

1 INTRODUCTION

Tailings is a rock flour produced as a by-product of mineral extraction. It is hydraulically transported, deposited above or under water and stored in man-made reservoirs called Tailings Storage Facilities (TSF). The stability of TSFs depends on the strength of this loose granular material which, when saturated, is prone to static liquefaction. As the construction is carried out in stages over several years, tailings may be deposited under widely varying conditions. Immediately after deposition, each layer may end up with a different initial moisture content (ω_0), degree of saturation (S_w), void ratio (e_0) and state parameter (ψ_0), etc. Moreover, there might be variations in mineral content and particle size. Post-depositional exposure to climate influences evaporation, vertical flow, desaturation, volume changes and cracking, re-saturation upon wetting from subsequent raises, etc.

FEM analyses of an entire TSF may lead to computationally expensive models, as the distance between the deposition point and the edge of the TSF may be in the range of kilometres. In the initial design stages, all what is needed is to identify if a given deposition strategy may result in weak layers posing high risk of instability due to static liquefaction. As most of the post-depositional processes are essentially 1D, the infinite-slope problem, relevant to the stability of the beach and far from the external slope, can be analysed in a 1D soil column (Figure 1).

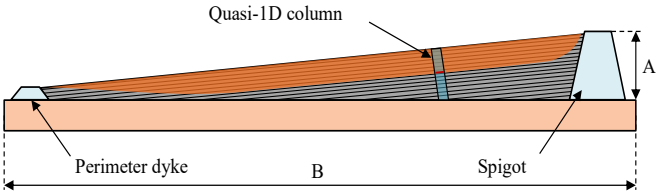

Figure 1: Schematic TSF and a Quasi-1D column analysis. Distance B can be easily 10 to 50 times higher than height A.

In this paper, the staged construction of a TSF and its stability is analysed at screening level in a quasi-1D column through a Python script and Plaxis FEM software. The critical state NorSand constitutive model (Jefferies, 1993) and Bishop´s effective stress for unsaturated soils are used to simulate the stress path during construction and stability analyses.

2 STATEMENT OF THE PROBLEM

A conceptual cartoon of the stress path of a given layer of tailings during the construction of a TSF is shown in Figure 2. The sequence is: A) saturated tailings are deposited; B-C) tailings flow downslope (a critical state flow, point B is on the critical state line CSL); flow stops, and the tailings surface is exposed to climate, inducing evaporation, downwards seepage, shrinkage

and overconsolidation; C-D) tailings become unsaturated and shrink maybe down to the shrinkage limit; cracking leads to a steep increase in vertical hydraulic conductivity; D-E) the burden of new layers produces oedometric recompression, resaturation and maybe primary compression depending on the height of the pile, the water availability and the air entry value of the tailings. This stress path is, essentially, a 1D process entailing vertical water flow, oedometric compression and 1D consolidation. It is however interesting to note that the tailings undergo changes from the contractive to the dilative zones and back (right to left, and left to right of the CSL in Figure 2).

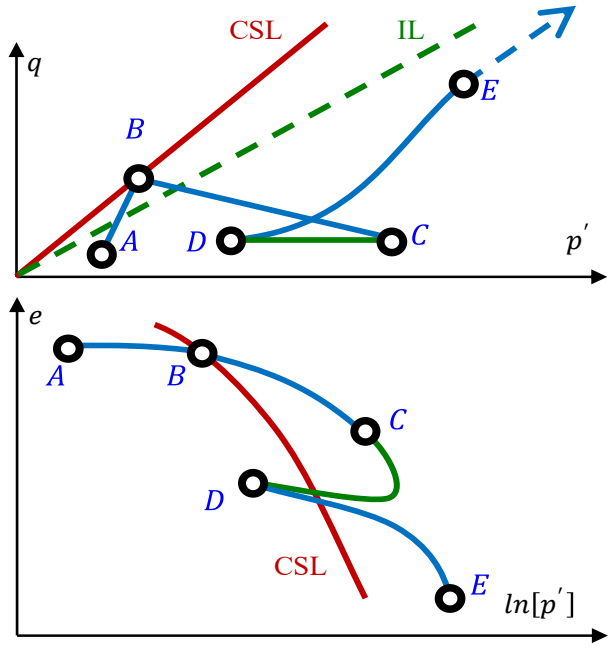

Figure 2: Stress path of tailings in the construction phase.

The $e - p'$ path C-D bending backwards in the lower half of Figure 2 is the result of the tailings going into unsaturated state. Bishop´s effective stress

$$p' = p + S_e \cdot s \qquad (1)$$

where p is total mean pressure, s is suction,

$$S_e = (S_{sat} - S_w)/(S_{sat} - S_{res}) \qquad (2)$$

is the effective saturation, S_{sat} and S_{res} are the degrees of saturation at saturated and residual states from the SWCC. Therefore, the maximum value of p' in the C-D path is reached where $S_e \cdot s$ is maximized; if the tailings get dry, $S_w \to S_{res}$, $S_e \to 0$, and $p' \to p$.

The problem gets more complicated due to differences in tailings grain size, water content at deposition, distance from deposition points and climate. Also, heavy desiccation creates hydraulic barriers limiting the downwards flow of supernatant water from fresh tailings, and therefore interbedded unsaturated and saturated layers may be produced.

The resulting tailings body is a very loose sloping ground formed by a material that can be strain-softening and brittle. Any perturbation of the equilibrium of this tailings body might induce a surface instability, where part of the ground mass slides down in an “infinite slope” motion until a flatter stable surface is attained. If not properly analyzed, this motion migth result in the release of tailins. The evaluation of the risk of such failure is the objective of this study.

3 QUASI-1D TAILINGS COLUMN

Post-deposition processes, as described in Section 2, are essentially 1D, and can therefore be analysed employing a quasi-1D model. In this paper, the modelelling starts from the point E at Figure 2. Figure 3 illustrates the sequence: drained staged construction is followed by an undrained pushover analysis enforcing uniform average shear strain in the full tailings column.

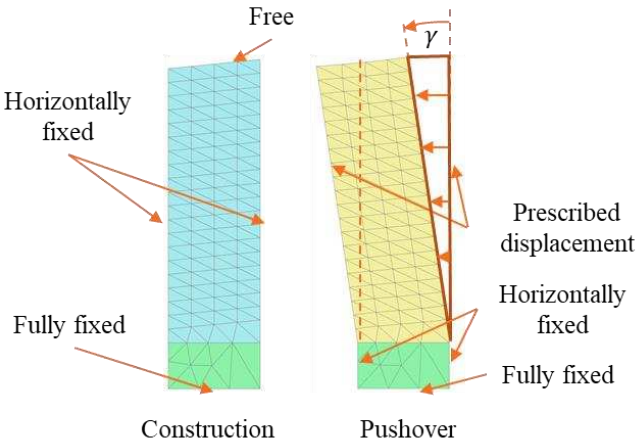

Figure 3: Quasi-1D analysis of a TSF column.

Figure 4 illustrates a conceptual result: the total horizontal force ΣF_x required to maintain a uniform distortion changes its sign during the pushover analysis: it starts as negative (to the right), flips to a maximum positive value as the column is pushed, and eventually changes sign again.

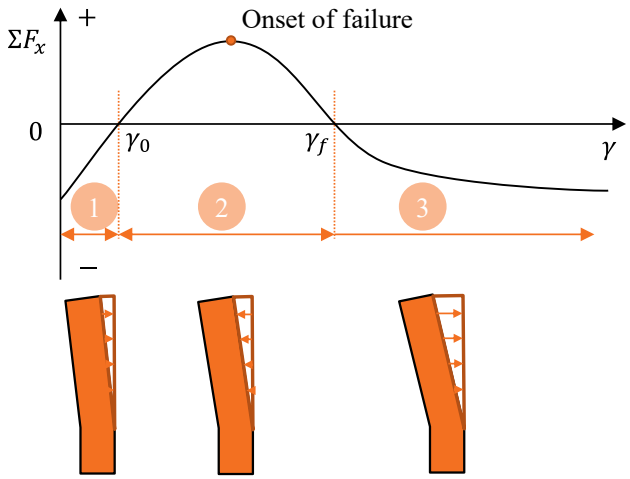

Figure 4: Interpretation of the pushover analysis.

The reasons for this behaviour are as follows: with no external loads, and due to the surface slope, the column tends to move to the left to attain equilibrum. As the lateral displacements are prescribed, the reaction points to the right, defining Region 1 in Figure 4. When the self-equilibrium is reached, reaction forces vanish ($\Sigma F_x = 0$), defining the boundary between Region 1 and Region 2 at a distortion γ_0. In Region 2, an additional force is required to push the column to the left until the peak strength is attained at some layer. This region may end at a point where the column is no longer available to resist the displacement (due to strain softening), and hence is no longer stable ($\Sigma F_x = 0$ again). This condition defines the boundary between Region 2 and Region 3 at a distortion γ_f. After this point, the column must be supported by an external force, defining Region 3. The curve tends to a final ΣF_x determined by the residual undrained shear strength of the weak layers in the tailings body. Sometimes, γ_f is not reached, as the residual strength is enough to balance the column itself.

The peak of the $\Sigma F_x - \gamma$ curve marks the onset of strain localization at the weakest layer. Therefore, the analysis provides the location of the weakest layer, its peak and residual undrained shear strength and the distortion of the full column required to initiate progressive failure.

As most variables are only bracketed into wide ranges at design stage, a statistical approach is employed, where multiple realizations are performed by means of a Python script implemmented in PLAXIS 2D®.

4 NORSAND CONSTITUTIVE MODEL

NorSand is a critical state constitutive model well-known in the industry and frequently used to simulate static liquefaction of tailings. In NorSand, the state of a soil is determined by two state variables. The first one is the state parameter

$$\psi = e - e_c \tag{3}$$

where e is the void ratio and e_c is the critical state void ratio at the current mean effective pressure. The second state variable is the image pressure p_{im}, the mean effective pressure at which the volumetric plastic strain rate is zero ($\dot{\varepsilon}_v^p = 0$). For details of the NorSand constitutive model see (Jefferies, 1993) (Jefferies & Been, 2016). While the focus of this paper is not NorSand, a few comments are provided to explain the influence of some parameters in the modelling.

The first observation is related to the simulation of a realistic post-construction stress field. During the deposition stages of the various layers, the tailings body essentially follows an oedometric stress path

$$\dot{\sigma}_3' = K_0 \cdot \dot{\sigma}_1' \tag{4}$$

The actual value of K_0 plays a major role in static liquefaction analyses, as minor changes in K_0 result in significant changes in the resulting brittleness of the material when subjected to undrained shearing, see for example (Fourie & Tshabalala, 2005). Therefore, it is of high importance that, at the end of the construction stages, a realistic stress field (a realistic K_0), void ratio and pore pressure field be achieved at all points in the model.

As NorSand employs only one yield function, inherited from the Original Cam Clay model, and uses associative plasticity, it is rarely possible to calibrate a single set of material parameters that would realistically reproduce the experimental behavior for both a K_0 stress path and an undrained shear ($\dot{\varepsilon}_v = 0$) stress path (Federico, et al., 2009). To yield a reasonable value of K_0 during the construction stages, a very high value of M_{cv} is required (Figure 5).

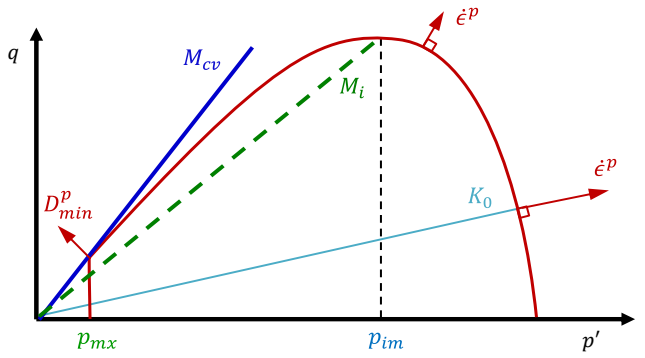

Figure 5: NorSand yield surface, calibrated for oedometric (K_0) compression stress path.

After the construction stages are completed, a lower realistic value of M_{cv} must be employed to simulate the shear stress paths that prevail during the pushover analyses. This reduction of M_{cv} induces plasticity and a stress redistribution which in turn increases K_0. In the calibration procedure used in this study, the image stress p_{im} is increased at the same time that M_{cv} is reduced to keep the target value of K_0 and the stresses lying on the yield surface.

In this study, a straight critical state locus (CSL) in $\ln(p') - e$ space

$$e = \Gamma - \lambda_e \cdot ln\left(p'/p_{ref}\right) \tag{5}$$

is employed, where Γ and λ_e are material parameters and p_{ref} is a reference pressure.

5 SIMPLE EXAMPLE

The simplest case is shown below, where a set of layers are built slow enough to allow for full equilibrium of

pore pressures. The point of rotation can occur at any height within the column. In the simple case shown here, a constant distortion is monotincally applied to the full column up to $\gamma = 10\%$.

5.1 Input data

The column has a total height $H_t = 60\ m$, a superficial tailings slope $\beta = 10\%$, a width $B = 10\ m$, and is divided into layers of uniform thickness. The water table is set at 30% and 60% of H_t and flow is restricted in lateral and bottom boundaries. NorSand parameters are shown in Table 1. The reader is referred to (Jefferies & Been, 2016) for a definition of the various parameters. The PLAXIS 2D® Hypres Van Genuchten Soil Water Characteristic Curve for a fine subsoil is employed to account for the computation of Bishop´s stresses in the unsaturated region.

Table 1. NorSand parameters.

G_{ref}	p_{ref}	n_G	ν	Γ	λ_e	ψ_0
20 MPa	100 kPa	4	0.2	1	0.06	-0.1
M_{cv}	N	χ_{tc}	H_0	H_ψ	R	S
1.7 | 1.3	0.35	4	300	0	1	1

The two values of M_{cv} shown in Table 1 correspond to the calibration for oedometric ($M_{cv} = 1.7$) and undrained shear stress paths ($M_{cv} = 1.3$). The former is required to attain $K_0 \approx 0.65$ as shown in Figure 6.

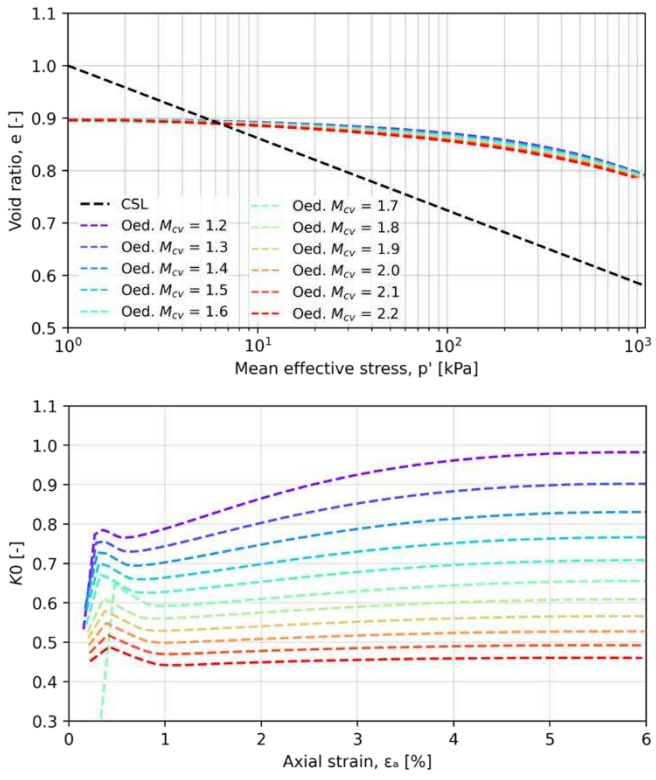

Figure 6: M_{cv} influence on K_0 for an oedometric stress path.

5.2 Construction stages

At each construction stage, the various processes can be simulated as follows:

- For a given layer, a set of material parameters, state variables, layer thickness and construction rate are selected from the corresponding probability density function of each variable.
- The layer is activated in a fully coupled flow-deformation stage; the initial conditions are full saturation and the at-deposition void ratio; the activation period matches the rate of raise of the layer, self-weight consolidation is allowed to occur.
- Interaction with the climate is simulated by imposing an evaporation or infiltration flow rate at the surface; equilibrium of the pore pressure field may induce desaturation and/or flow from or to the layers below; at this stage, cracking and changes in hydraulic conductivity could be incorporated to the simulation.
- A new layer is activated, inducing coupled flow and deformation of all the previous layers in the column; a water table may be created in the process.

5.3 Pushover analysis

After the construction is completed, NorSand parameters are updated and the material is switched to undrained. A distortion γ is imposed by linear displacements on lateral sides of the column (Figure 3); boundary vertical displacements are restricted.

Figure 7 shows three meshes with different layer heights: $5.0\ m$, $1.5\ m$ and $0.5\ m$. Being an uniform material, layer height should have no impact, and is therefore used here to study mesh-dependency. The resulting obliquity ($\eta = q/p'$) and void ratio e are presented for each column. Other numerical aspects of this study are presented at (López Rivarola, et al., 2022).

5.4 Results

During the construction stages, no strain-softening occurs, no mesh dependency is observed, and all three models result in similar stress fields and void ratios, as shown in Figure 7. However, some numerical noise can be observed in the results of the coarser mesh. Figure 8 shows the results obtained in the pushover analysis of the three models.

The distortion at the onset of failure is about the same for the three meshes ($\gamma \cong 0.4\%$, see Figure 8). The total load required to fail the column is the same for the medium and fine meshes, but is significantly higher for the coarser mesh. This mild mesh-dependency has been confirmed with additional runs: elements finer than a threshold produce results, in terms of distortion at the onset of failure and total load, that converge to stabilized values (i.e. mesh-dependency is not entirely pathological).

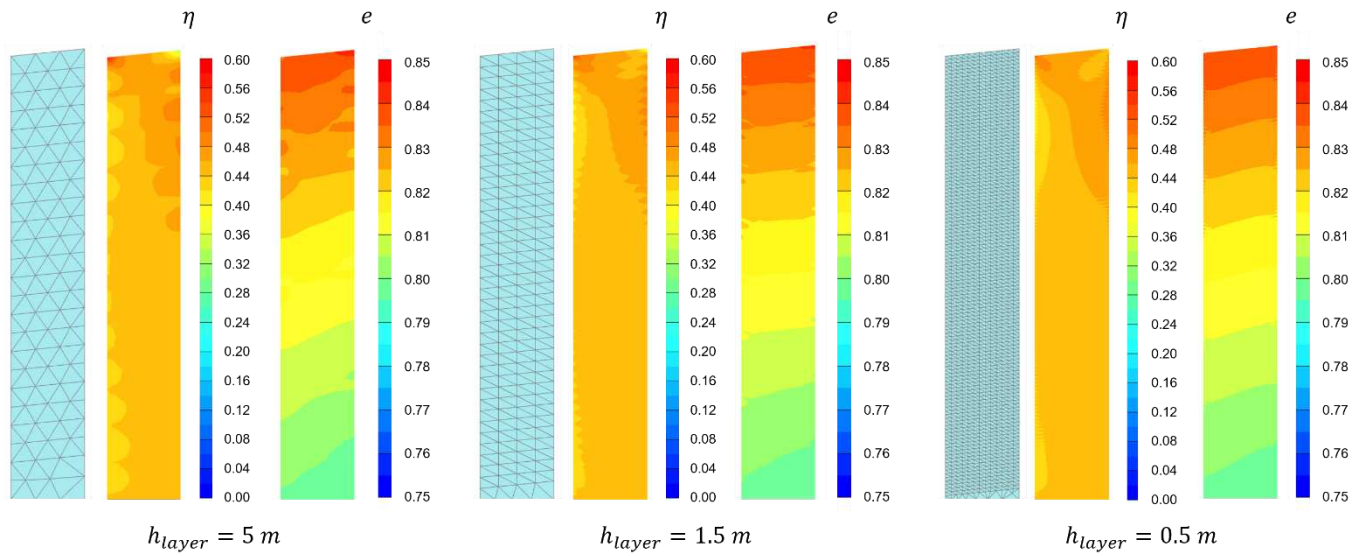

Figure 7: Final configuration of construction phases for three different layer heights.

From the model having $h_{layer} = 1.5\ m$, a second model is created by introducing a weak layer. This weak layer has the same material parameters of the rest of the tailings column (as shown in Table 1), except for the initial state parameter which is set at $\psi_0 = 0.0$, a higher value compared to $\psi_0 = -0.1$ that yields both lower peak and residual undrained shear strengths. The results $\Sigma F_x - \gamma$ are shown in Figure 9 for both models.

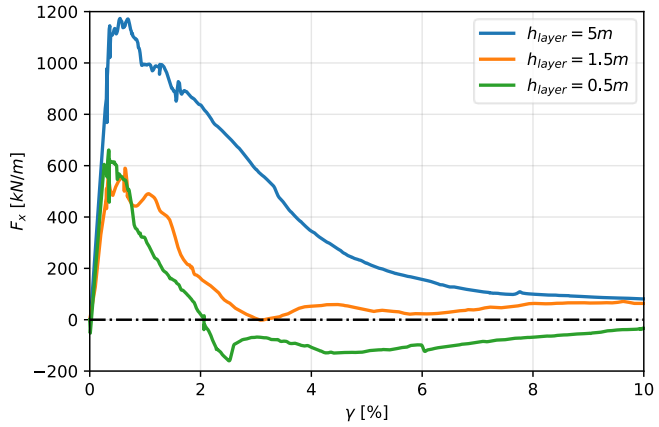

Figure 8: Pushover curves for the three meshes.

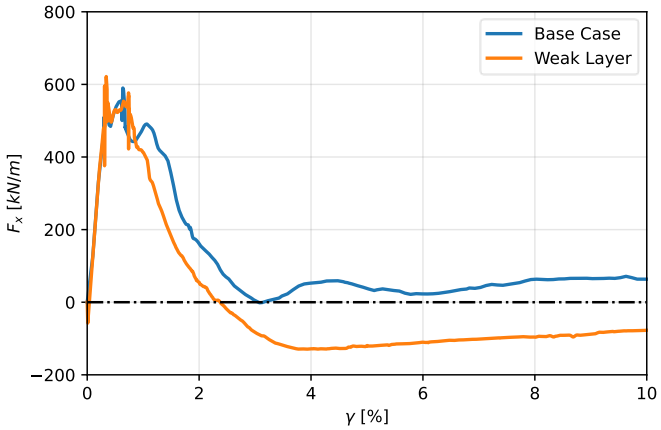

Figure 9: Pushover curves: base case and weak layer models.

A few conclusions can be drawn from these curves: i) the max value of $\Sigma F_x = 600\ kN/m$ and the distortion at the onset of failure $\gamma \cong 0.2\%$ are the same in both models; ii) the base case does not reach Region 3 in Figure 3, the residual undrained strength is enough to equilibrate the column; iii) in the model with the weak layer, strain localization in the weak layer is fully developed at about $\gamma \approx 0.6\%$; however, the model only gets into Region 3 at a deformation of about $\gamma = 2.4\%$, when the bottom layer reaches full softening.

Figure 10 shows the deviatoric strain contours for both models for $\gamma = 0.2\%|0.6\%|10\%$. It is observed that, in the base case, strain localization in the form of a circular failure surface at the bottom of the model (a hinge) is observed at large distortion. On the other hand, the model with the weak layer shows a clear horizontal and also a vertical localization line, for a small distortion $\gamma = 0.6\%$.

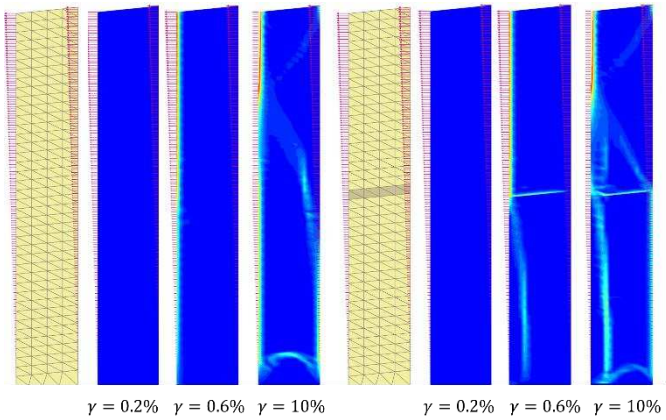

Figure 10: Stress localization at various deviatoric strains. (a) base case. (b) weak layer.

6 USE OF THE QUASI-1D COLUMN IN THE PRELIMINARY DESIGN OF A TSF

The quasi-1D column may be employed in the preliminary design stages of a TSF as follows:

- Design variables are selected as aleatory variables; a probability density function is calibrated for each variable. Some variables are heavily correlated, for instance the superficial slope angle and the at-deposition water content. Others, like climate or changes in the material properties, are assumed uncorrelated aleatory variables.
- A number of realizations of the quasi-1D model are performed, in an atempt to identify which are the values of the key variables that drive the column into Region 3 of Figure 3. This is an indicator that, should yielding be initiated, it would not be contained and arrested, but would fully develop an infinite planar failure surface.
- Threshold values of the key parameters are reported, e.g. the max admisible water content at deposition, which turns out to be a function of the depth of the particular layer within the tailings body.

7 CONCLUSIONS

A procedure to perform stability analyses of tailings storage facilities by means of a quasi-1D column is presented. The procedure is intended to be used for deposits built in layers and to be run at the early design stages of a TSF, where the main purpose is to identify if a given deposition strategy may result in weak layers posing high risk of instability due to static liquefaction, and when a full FEM study is not yet appropriate.

Within the quasi-1D soil column, a fully coupled flow-deformation numerical strategy employing the critical state constitutive model NorSand and Bishop stress is employed to simulate the various processes that occur during the construction of the embankment, including 1D compression, consolidation, evaporation, unsaturation and resaturation of the various layers of tailings.

All relevant variables are assumed to be aleatory, and therefore the quasi-1D model is intended to be run many times. This is achieved at a reasonable cost by a Python script in PLAXIS 2D®.

The result of each analysis is a load-distortion curve which informs the distortion at the onset of failure and whether the fully softened column would resist its own weight.

Should the column require external forces to resist its own weight after a large distortion is applied, this is an indicator of risk of progressive failure and uncontained flow.

A simple example is given to demonstrate how the procedure works. First, an homogeneous tailings body is simulated. Then, the model is perturbated by inserting a weak layer. A comparison between the results of both models is given, showing the difference between a result that would be read as a stable configuration, and one that would be read as leading to uncontained flow.

8 ACKNOWLEDGEMENTS

The authors wish to acknowledge the support of the team at the University of Buenos Aires and SRK Consulting during the development and testing of the models presented in this paper. Special appreciations go to Arcesio Lizcano, Osvaldo Ledesma, and Mauro Sottile for their useful comments and fruitful discussions.

9 REFERENCES

Federico, A., Elia, G., Murianni, A. 2009. The at-rest earth pressure coefficient prediction using simple elasto-plastic constitutive models. *Computers and Geotechnics* **36**, 187-198.

Fourie, A.B., Tshabalala, L. 2005. Initiation of static liquefaction and the role of K0 consolidation. *Canadian Geotechnical Journal* **42**, 892-906.

Jefferies, M.G. 1993. Nor-Sand: A simple critical state model for sand. *Géotechnique* **43(1)**, 91-103.

Jefferies, M.G., Been, K. 2016. *Soil Liquefaction - A critical state approach*. Second Edition (2nd ed.). CRC Press, London.

Rivarola, F.L., Tasso, N., Bernardo, K., Sfriso, A. 2022. Numerical aspects in the evaluation of triggering of static liquefaction using the HSS model. *Mecánica Computacional* **XXXIX**, 983-992.